

The British University in Egypt

BUE Scholar

Chemical Engineering

Engineering

2018

Performance of Nanoporous Carbon Membrane for Hydrogen Recovery

Abdulrahman A. Al-Rabiah
King Saud University, arabiah@ksu.edu.sa

AbdelHamid M. Ajbar
King Saud University

Moustafa A. Soliman
The British University in Egypt, moustafa.aly@bue.edu.eg

Omar Y. Abdelaziz
Lund University

Follow this and additional works at: https://buescholar.bue.edu.eg/chem_eng



Part of the [Membrane Science Commons](#)

Recommended Citation

Al-Rabiah, Abdulrahman A.; Ajbar, AbdelHamid M.; Soliman, Moustafa A.; and Abdelaziz, Omar Y., "Performance of Nanoporous Carbon Membrane for Hydrogen Recovery" (2018). *Chemical Engineering*. 82.

https://buescholar.bue.edu.eg/chem_eng/82

This Article is brought to you for free and open access by the Engineering at BUE Scholar. It has been accepted for inclusion in Chemical Engineering by an authorized administrator of BUE Scholar. For more information, please contact bue.scholar@gmail.com.

Performance of Nanoporous Carbon Membrane for Hydrogen Recovery

¹Abdulrahman A. Al-Rabiah*, ¹Abdelhamid M. Ajbar, ²Moustafa A. Soliman, ^{3,4}Omar Y. Abdelaziz

¹Chemical Engineering Department, King Saud University, Riyadh 11421, Saudi Arabia.

²Department of Chemical Engineering, The British University in Egypt, Cairo 11837, Egypt.

³Department of Chemical Engineering, Cairo University, Giza 12613, Egypt.

⁴Department of Chemical Engineering, Lund University, P.O. Box 124, SE-221 00 Lund, Sweden.
arabiah@ksu.edu.sa*

(Received on 10th January 2017, accepted in revised form 13th October 2017)

Summary: The aim of this work is to study the performance of nanoporous carbon membrane for hydrogen recovery from off-gas streams. The study is based on a rigorous mathematical model which can predict the performance of nanoporous selective surface flow (SSF) carbon membrane. Basically, the developed model is based on two transport mechanisms: the dusty gas flow through porous media and the surface adsorption-diffusion. The model was employed to simulate the hydrogen recovery from off-gas stream using SSF carbon membrane at different operating conditions. The separation performance of hydrogen-hydrocarbon mixture by nanoporous carbon membrane was evaluated and described. A comparison between the model simulation and the experimental data related to hydrogen recovery from off-gas streams shows good agreement. A parametric study is further carried out to show the effects of pressure at the membrane feed and permeate sides. The effects of flow-rate and type of sweep gas at the membrane permeate side on hydrogen recovery are also shown. SSF membrane illustrates a significant potential to be used for hydrogen recovery from refinery off-gas streams.

Keywords: Hydrogen production, Membranes, Dusty gas model, Hydrogen-hydrocarbon separation, Selective surface flow, Hydrogen gas transport

Introduction

Hydrogen is considered as an important chemical in conventional petroleum refineries [1] and other chemical plants producing ammonia and methanol [2] as well as in renewable resources [3]. Hydrogen economy emerged as a potential solution that could address problems related to energy security, global warming, and air pollution. In this way, hydrogen is obviously becoming a principal component within the future energy mix. Therefore, research should be directed towards improving and developing efficient methods for hydrogen production, separation, and purification.

Hydrogen separation from other associated gases is an essential step within the process of hydrogen production. In order for hydrogen to be used further, it should be separated from those gases/impurities that accompany it inevitably. Commercially available separation technologies, such as cryogenic/fractional distillation and pressure swing adsorption (PSA), are normally adopted for hydrogen recovery, albeit, their energy intensive nature is the main drawback [4]. Water electrolysis is another promising methodology/approach for large-scale hydrogen production, comprising the cathodic hydrogen evolution reaction (HER) and the anodic oxygen evolution reaction (OER) [5, 6]. Membrane separation processes are also used to recover

hydrogen with high purity, while less energy requirement is needed. Moreover, it offers possibility for easy and continuous operation, making it a cost effective process [7]. Thus, it is considered to be an attractive alternative compared to other commercially available technologies.

Membrane technology has been receiving increasing attention in the last two decades for the separation of liquids and gases [8–10]. The membrane technology represents a good solution for the application in large-scale separations due to ease of operation, low capital and operating costs, low energy consumption, and high packing density [11]. A number of current industrial applications such as hydrogen recovery from refinery process, nitrogen removal from natural gas, and oxygen enrichment could benefit from the membrane technology [12].

Indeed, literature is rich in studying the hydrogen production and separation using a plenty of different membrane types and configurations [13, 14]. Pd–Ru membrane supported on a porous yttria-stabilized-zirconia/stainless steel substrate was adopted to produce hydrogen through steam methane reforming with the aid of a commercial Ni-based reforming catalyst [15]. A high purity level of hydrogen was attained within an actual syngas

*To whom all correspondence should be addressed.

atmosphere, derived from a coal gasification unit, using composite Pd and Pd-Au membranes [16]. It is crucial in those syngas operations to separate both H₂ and CO₂ necessary for hydrogen production, especially in refineries, petrochemical complexes, and recently in integrated gasification combined cycle (IGCC) plants [17], [18]. This issue has been addressed latterly by Lin et al. in their recently published two-part paper, describing the process of membrane development and including techno-economic analyses for different process designs [19], [20]. In another example, the effect of gases including CO₂, N₂, and H₂O on hydrogen permeation was investigated using a Pd-based membrane [21]. The optimum operating conditions for hydrogen separation from the mixtures were identified and the inhibition factors towards permeability were determined. Ultrathin graphene oxide membranes, with typical thickness of 1.8 nm, showed a high H₂/CO₂ and H₂/N₂ mixture separation selectivities performance, introducing an attractive option for practical hydrogen separation from mixtures [22]. In another hydrogen separation application, supported carbon molecular sieve membrane was studied to determine the selectivity and permeation properties for low molecular weight gases, presenting a competitive alternative in gas separation [23].

Carbon-based membranes appeared to be an efficient approach for hydrogen separation and purification via hydrogen rejection and contaminate permeation [7]. Other types of hydrogen selective membranes available based on the used material are: polymeric, metallic, and ceramic. Examples of investigated novel carbon materials include K-doped graphene (K-GS) [24], cuprous oxide nanowires decorated graphene oxide nanosheets (Cu₂O-GO) nanocomposites [25], aminated/carboxyl graphene quantum dots [26], and carboxylic graphene quenching probe [27]. In addition, its applications extend to include separation and purification of other gases such as nitrogen [28, 29] and carbon dioxide [30]. Porous materials, in particular, among different others received a great attention for various chemical technology and separation applications involving purifications of gaseous mixtures [31]. This is evidently due to their operational simplicity, low capital and operation costs, and high performance efficiency. In 1993, Rao and Sircar presented new nanoporous carbon membranes for separation of gas mixtures and they called them Selective Surface Flow membranes (SSF) [32, 33]. Those membranes offer efficient hydrogen separation, by hindering the hydrogen pore diffusion through the selective adsorption of hydrocarbons. For a hydrogen-hydrocarbons gas mixture, hydrocarbons are

preferentially adsorbed and transported across the membrane, while hydrogen is enriched on the feed side. This is an important advantage of the SSF membrane since the desired product (i.e. hydrogen) is obtained at the retentate, avoiding recompression. This comes in contrast to the molecular sieving membrane where the small hydrogen molecules pass preferentially through the small pores of the membrane to the permeate side [34]. Basically, the surface nature and the pore size highly affect the membrane performance. Fine-tuning through different synthetic methods and optimization have led to numerous advantages in gas separation, like hydrogen purification. Currently, research efforts are ongoing in the field towards enhancing the efficiency and the performance of these membranes [35, 36].

The objective of this work is to tackle our developed model of the SSF from a classical perspective using the dusty gas theory for hydrogen production and performance prediction. The results of our developed model for nitrogen separation are compared with the work of Rao and Sircar [37] for the separation of hydrogen-hydrocarbons gas mixtures. Rao and Sircar's model is based on Fick's law and is thus considered over simplification. This study shows that our previously developed model can also be used when the operating parameters are varied and the application is differed. First, the paper illustrates the hydrogen gas transport mechanism through SSF membranes. Then, the model is briefly described where the model solution is based on the orthogonal collocation approach. This is followed by the results and discussion section, where a comparison between model simulation and experimental results are made. A parametric study and observations are finally presented and drawn for hydrogen recovery.

Theory

SSF membrane could be utilized in recovering the hydrogen gas from refinery waste streams. This type of membrane can efficiently produce hydrogen as an enriched stream from refinery spent gases by selectively permeating the hydrocarbons through the membrane. Fig. 1a depicts a schematic of a selective service flow membrane, describing the selective adsorption-surface-diffusion-desorption mechanism for separation of gas mixtures. Normally, the membrane can be formed within the support pores or on its surface. The Fig also describes the mechanism of gas transport for separation of hydrogen-hydrocarbon mixture. The gaseous mixture feed enters from the high pressure side over the surface of the membrane, while the other membrane

side is maintained at a lower pressure. Selective adsorption of the larger and the more polar molecules (hydrocarbon molecules) hence occurs onto the pores over hydrogen gas. Further, diffusion of the adsorbed molecules takes place on the surface towards the membrane low pressure side, where they afterwards desorb forming the permeate stream. The adsorbed molecules consequently hinder and block the flow of the non-adsorbed components of the gaseous mixture feed via the void space between the pore walls. Accordingly, the hydrogen-rich product is produced

on the membrane high pressure side and the hydrocarbon-rich waste is produced at the membrane low pressure side. In addition, Fig. 1b shows a typical scanning electron micrograph image of a five-coated carbon membrane that was measured using a magnification of 20,000, as proposed within Rao and Sircar research in order to illustrate the module morphology. It may be seen that the membrane consists of five uniform layers of carbon without any visible cracks.

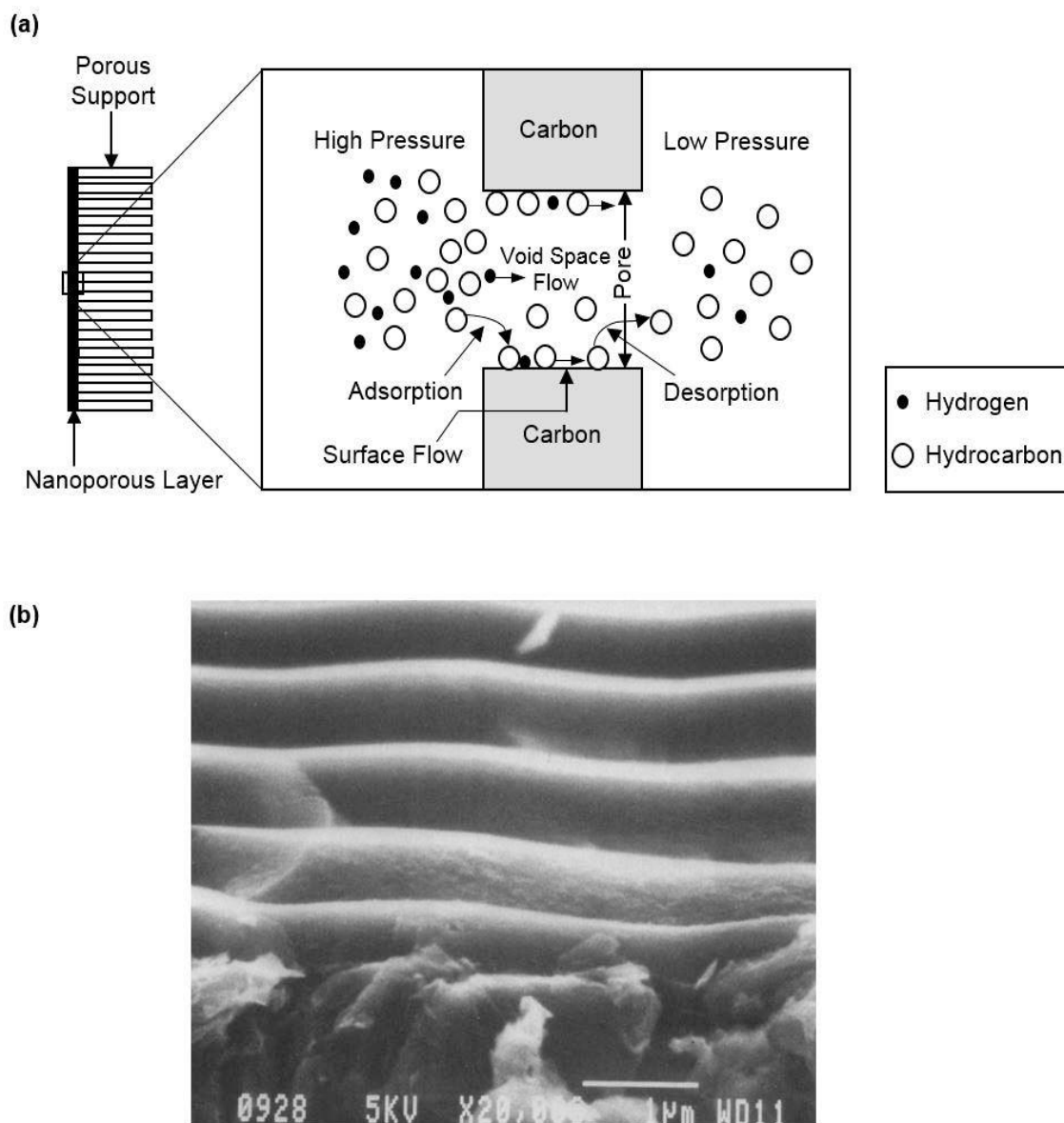


Fig. 1: Gas transport mechanism through SSF nanoporous carbon membrane (a) and a typical scanning electron micrograph of a nanoporous five-coated carbon membrane, adopted from Rao and Sircar research (b).

Methodology

We adopt the model that we previously developed to predict the transport of different species of multi-component gas mixture through the nanoporous carbon membranes and applied for nitrogen separation [29]. Here, the model is employed to highlight its capability and applied for predicting the performance of hydrogen recovery, in particular, via SSF membranes. Briefly, four different modes of transport existing in porous media are incorporated within the model, namely, Knudsen flow, bulk/viscous flow, ordinary diffusion, and surface flow and we consider a similar schematic diagram for the counter-current flow membrane used previously by Shindo et al. [38] for approaching the simple solution-diffusion model, as shown in Fig. 2.

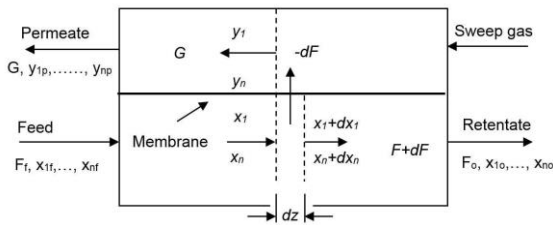


Fig. 2: Schematic of membrane flow diagram with counter-current configuration.

Main assumptions involved within the mathematical model are outlined as follows:

- The permeability of each gas component is assumed to be independent of the pressure and temperature. The system is isothermal and the pressure is constant along the feed side. So, any deviation from this assumption will not affect the results.
- The membrane thickness is assumed to be constant along the length of the unit.
- Pressure drops of the feed and permeate gas streams are negligible. This is reasonable because there is no change in the total number of gas moles.
- A plug flow is assumed to prevail in the feed and permeate streams; it is appropriate for high velocity flow.

The balance equations for each component are stated as:

$$\frac{dF_i}{dA} = -NT_i, \quad F_i(0) = Fy_i(0) \quad i = 1, 2, n \quad (1)$$

$$\frac{dG_i}{dA} = -NT_i, G_i(A_T) \text{ given} \quad i = 1, 2, n \quad (2)$$

whereas F_f is the inlet feed flowrate, F_i is the flowrate of component (i) in retentate, NT_i is the total flux through the membrane of component (i), G_i is the flowrate of component (i) in the permeate, y_i is the gas mole fraction at the permeate side, A_T is the membrane area, and $G_i(A_T)$ is the inlet permeate side flowrate for component (i) at the total area A_T (sweep gas).

The total flux (NT_i) is the sum of the dusty flux (N_i) and the surface diffusion flux (NSD_i) as shown in the following equation:

$$NT_i = N_i + NSD_i \quad (3)$$

The dusty gas model equations are given as:

$$-\sum_{j=1}^n \frac{(x_j N_i - x_i N_j)}{D_{ij}^K} - \frac{N_i}{D_i^K} = \frac{P}{RTL} \frac{dx_i}{dz} + \frac{x_i}{RTL} \left(1 + \frac{\epsilon r^2}{8} \frac{P}{\mu_i D_i^K}\right) \frac{dP}{dz} \quad i = 1, 2, n$$

(4)

where L is the thickness of the membrane, z is the dimensionless distance through the membrane, P is the total pressure inside the membrane, T is the temperature, x_i is the mole fraction inside the membrane, D_i^K is the Knudsen diffusivity, D_{ij} is the binary gas diffusivity, r is the pore radius, and μ_i is the gas viscosity.

The model equations are solved using the orthogonal collocation method [39]. The orthogonal collocation is applied at n_c interior collocation points inside the membrane such that:

$$\frac{dx_{i,j}}{dz} = \sum_{k=2}^{n_c+1} A_{j+1,k} x_{i,k-1} + A_{j+1,1} y_i \quad j = 1, 2, n_c \quad \text{and} \quad i = 1, 2, \dots, n \quad (5)$$

There are $(n \times n_c)$ variables: $x(i+(j-1)n)$ $i=1, 2, \dots, n$ and $j=1, 2, \dots, n_c$ where i represents certain component and j represents collocation point. $A_{j,k}$ are the elements of $((n_c+1)(n_c+1))$ matrix of the weights of first derivative. In the same way, for the pressures:

$$\frac{dP_j}{dz} = \sum_{k=2}^{n_c+1} A_{j+1,k} P_{k-1} + A_{j+1,1} P_F \quad j = 1, 2, n_c \quad (6)$$

Such that P_F is the pressure at feed side and P_k equals $x(nn_c+k)$, $k=1, 2, \dots, n_c$. The mole fractions (m_i) of the gas at the permeate side are required to be equal to those obtained from extrapolation of the mole

fraction of the gas at the feed side and the membrane, such that:

$$m_i = \sum_{k=1}^{nc+1} (X_{interp})_k x_{i,k-1} + (X_{interp})_1 y_i \quad i = 1, 2, n-1 \quad (7)$$

Where $(X_{interp})_k$ are the elements of $(nc+1) \times 1$ vector of weights of the Lagrange interpolation formula at $z=L$.

Table-1 summarizes the values of the parameters used for the numerical simulation, especially employed for the hydrogen separation case. The values for the permeabilities are used to fit the experimental results ahead with Rao and Sircar's study [37], in order to account for the changes of permeabilities with gas composition. For more details on the solution strategy, readers are kindly referred to the aforementioned paper [29].

Table-1: Parameters used for numerical simulation.

Parameter	Value
Membrane thickness, L (μm)	2.5
Pore radius, r (Angstrom)	6
Hydrogen permeability, Q_{H_2} (barrers)	1.416
Methane permeability, Q_{CH_4} (barrers)	1.183
Ethane permeability, $Q_{C_2H_6}$ (barrers)	3.08
Propane permeability, $Q_{C_3H_8}$ (barrers)	7.874
Butane permeability, $Q_{C_4H_{10}}$ (barrers)	33.69

Results and Discussion

Since the mathematical model was initially solved and validated with a very good agreement with the experimental results, besides being applied on a nitrogen separation case study, it will therefore be adopted directly for the objective of hydrogen recovery. Moreover, the developed model appeared to be useful in carrying out performance analyses for the nanomembrane, making it also capable for carrying out parametric studies which will be presented in the latter sections.

Fig. 3a shows the variation of hydrogen recovery with its purity, for different feed pressures. The model predicts, as expected, a decreasing trend. As can be seen, the range of hydrogen recovery is between 90% and 100%, while the hydrogen purity is in the range of 40% to 46%. Also, for a required hydrogen recovery, an increase in the feed pressure increases the hydrogen purity. For example, at feed gas pressure of 3.38 atm, a recovery of 94% is associated with a hydrogen purity of 43.5 %, while at larger feed pressure of 5.11 atm, the purity increases to 44.4%. Fig. 3b presents the variations of hydrogen recovery with relative area, defined by the

permeability of the base component (hydrogen). Again, the model predicts the expected decreasing trend. For a desired recovery, the decrease in the feed pressure increases the required area. By way of illustration, for a hydrogen recovery of 94%, a decrease of feed pressure from 5.11 atm to 3.38 atm, increases the relative area from 0.24 to 0.42.

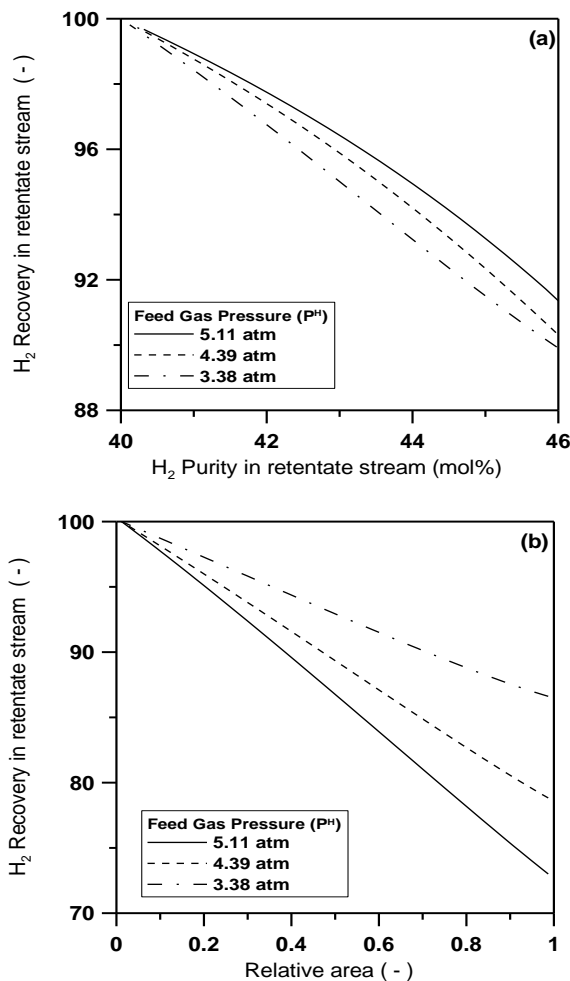


Fig. 3: Effect of feed gas pressure on SSF performance.

On the other hand, Table 2 displays the model predictions of the decrease in hydrogen sweep gas pressure from 1.48 to 1.07 atm. The ratio of sweep gas to feed flow rate is maintained at 0.05. It can be seen that, the model predicts that a decrease in hydrogen sweep gas pressures decreases the hydrogen recovery and the concentrations of the larger hydrocarbons. The evaluation of the relative error shows reasonable suitability of the model. The relative error for hydrogen recovery and the composition of smaller hydrocarbons is rather relatively small.

Table-2: Comparison between the model results and experimental data for different sweep gas pressures (feed gas pressure is 5.11 atm and ratio of hydrogen sweep gas to feed flow rate is 0.05).

Sweep gas pressure (atm)	Results	H ₂ Recovery(%)	H ₂ mol (%)	CH ₄ mol (%)	C ₂ H ₆ mol (%)	C ₃ H ₈ mol (%)	C ₄ H ₁₀ mol (%)
1.48	Experimental	81.3	49.2	23.4	19.2	6.7	1.54
1.07		77.1	50.5	23.9	19.8	5.6	0.16
1.48		75.4	51.1	25.2	17.7	4.9	1.03
1.07	Model results	71.9	52.3	26.3	17.3	3.9	0.22
1.48		7.3	10.4	3.9	7.8	26.9	33.1
1.07	Relative error (%)	6.7	0.4	3.6	12.6	30.4	37.5

Table-3: Comparison between the model results and the experimental data for different type and ratio of sweep to feed gas flow rates (feed gas pressure is 4.4 atm and sweep gas pressure is 1.07 atm).

Sweep to feed flow ratio	Results	H ₂ Recovery(%)	H ₂ mol (%)	CH ₄ mol (%)	C ₂ H ₆ mol (%)	C ₃ H ₈ mol (%)	C ₄ H ₁₀ mol (%)
		Hydrogen sweep					
0.14	Experimental	81.5	53.0	25.0	17.6	4.0	0.28
0.10		78.5	52.1	25.3	17.7	4.5	0.4
0.05		82.1	49.0	23.6	19.5	5.9	2.0
0.14		79.1	52.7	25.4	17.5	4.1	0.25
0.10		78.5	52.0	25.3	17.8	4.5	0.42
0.05	Model results	77.5	50.7	25.2	18.2	5.0	0.89
		2.9	0.6	1.6	0.6	2.5	10.7
	Relative error (%)	0.0	0.2	0.0	0.6	0.0	5.0
		5.6	3.5	6.8	6.7	15.3	55.5
		Methane sweep					
0.16	Experimental	70.1	52.9	27.3	16.5	3.3	0.0
0.10		70.3	51.5	26.0	17.6	4.3	0.44
0.05		71.0	50.0	25.0	18.7	5.3	0.81
0.16		72.3	48.7	29.6	17.5	4.0	0.19
0.10		72.9	48.7	28.7	17.8	4.5	0.41
0.05	Model results	73.7	48.5	27.4	18.2	5.0	0.86
		3.1	7.9	8.4	6.6	21.2	-
	Relative error (%)	3.7	5.4	10.4	1.1	4.7	6.8
		3.8	3.0	9.6	2.7	5.7	6.2

The model simulations for the performance of the nanomembrane are demonstrated in Fig. 4(a-b) for the conditions listed in Table 2. It is noticed from Fig. 4a that, for a given hydrogen recovery, a decrease in the sweep gas pressure increases the purity. On another hand, Fig. 4b shows that increasing the sweep gas pressure increases the required area. For instance, for hydrogen recovery of 90% the increase in hydrogen sweep gas pressure from 1.07 to 1.48 atm, subsequently increases the required relative area from 0.37 to 0.41.

Table 3 displays the model predictions for the effect of type and ratio of sweep to feed gas flow rate. In the experimental work, in one certain run, pure hydrogen was used as sweep gas with ratios to feed flow rate of 0.05, 0.10, and 0.14. In a second run, pure methane was used as sweep gas with ratios to feed flow rate of 0.05, 0.10, and 0.16. The feed gas and sweep gas pressures were maintained at 4.4 atm and 1.07 atm, respectively. It can be confirmed from Table 3 that, the model very well predicts the performance of the membrane for all the experimental values on hydrogen recovery.

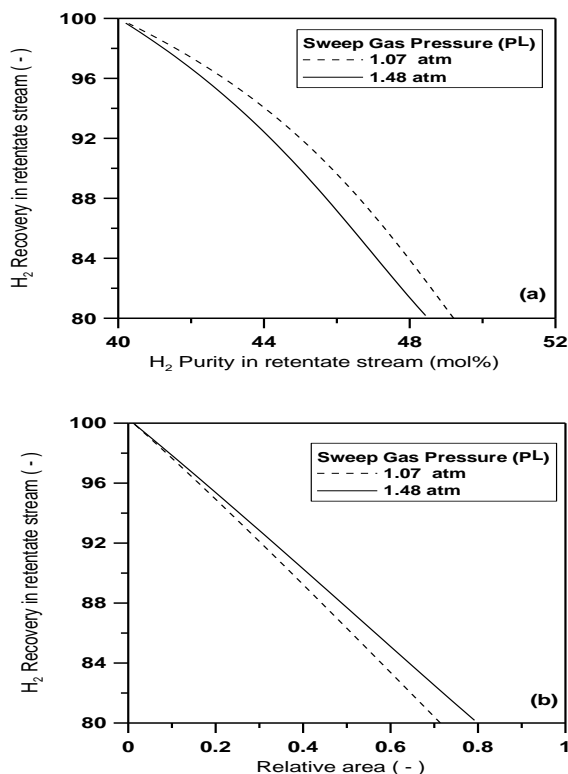


Fig. 4: Effect of hydrogen sweep gas pressure on SSF performance for the operating conditions of Table-2.

The model simulations pertinent to the case of using hydrogen as sweep gas are shown in Fig. 5(a-b). Fig. 5a demonstrates that for a given recovery, an increase in the ratio of sweep to feed gas increases the hydrogen purity. Nevertheless, Fig. 5b shows that for a given recovery, an increase in the hydrogen sweep ratio moderately increases the relative area.

When methane is used as sweep gas, a similar trend to that of hydrogen occurs (see Fig. 6a). On the contrary, Fig. 6b depicts an opposite trend in which an increase in methane sweep gas, decreases the relative area. It is worth mentioning that, the model is based on constant permeability of the gases through the membrane. As indicated by Rao and Sircar, the permeability changes with composition; this could explain any deviation in the results.

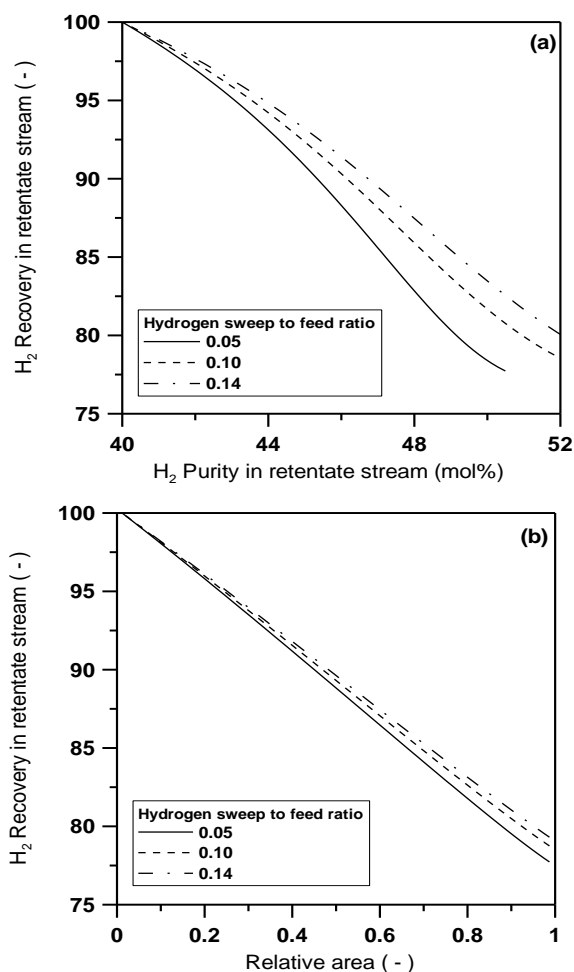


Fig. 5: Effect of hydrogen sweep to feed gas ratio on SSF performance for the operating conditions of Table-3.

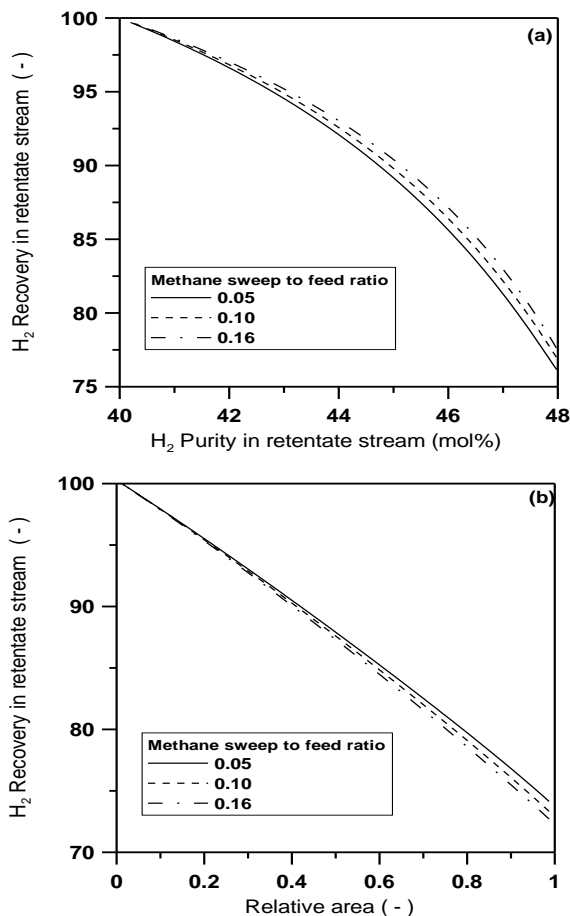


Fig. 6: Effect of methane sweep to feed gas ratio on SSF performance for the operating conditions of Table 3.

Conclusions

This study has introduced the application of a classical model that predicts the performance of nanoporous carbon membranes for hydrogen recovery, based on the dusty gas model and surface diffusion. The model was validated with experimental data for hydrogen-hydrocarbons separation and appeared to be useful for simulating the effect of various operating parameters on the performance of SSF membranes towards hydrogen production. The trends of the model predictions are consistent with other membrane performances reported in literature. The applied model can however be used in predicting the performance of nanoporous carbon membranes for other gas separation applications. Nanoporous carbon membranes hold a significant potential for recovering valuable chemicals (e.g., H₂) from industrial waste streams and further development, from a future perspective.

Nomenclature

A	membrane area (m^2)
A_T	total membrane area (m^2)
$A_{j,k}$	elements of the matrix of the weights of first derivative
D^K	Knudsen diffusivity (m^2/s)
D_{ij}	binary gas diffusivity (m^2/s)
F	inlet feed flowrate (mol/s)
G	flowrate in permeate (mol/s)
L	membrane thickness (m)
M	mole fractions at the permeate side
N	number of components
n_c	number of collocation points
N	dusty flux (mol/m^2s)
NSD	surface diffusion flux (mol/m^2s)
N_T	total flux through the membrane (mol/m^2s)
P	total pressure inside the membrane (Pa)
P_F	feed pressure (Pa)
P_H	pressure on feed side (Pa)
P_P	pressure on permeate side (Pa)
Q	permeability ($mol/s.m.Pa$)
r	pore radius (m)
R	universal gas constant ($J/mol K$)
s	dimensionless relative area
T	temperature (K)
x	mole fraction inside the membrane
X_{interp}	vector of weights of the Lagrange interpolation
y	gas mole fraction at the permeate side
z	dimensionless distance through the membrane

Greek

ε	porosity
μ	gas viscosity (kg/m.s)
τ	tortuosity

Subscripts

i,j,k	component index
M	base component
F	feed
H	feed side
P	permeate side

Acknowledgments

This work was made possible by a generous grant from King Abdullah Institute for Nanotechnology at King Saud University, Riyadh, Saudi Arabia..

References

- X. Wang, Z. Wang, H. Zhao and Z. Liu, A procedure for design of hydrogen networks with multiple contaminants, *Chinese J. Chem. Eng.*, **23**, 1536 (2015).
- J. Tallaksen, F. Bauer, C. Hulteberg, M. Reese and S. Ahlgren, Nitrogen fertilizers manufactured using wind power: greenhouse gas and energy balance of community-scale ammonia production, *J. Clean. Prod.*, **107**, 626 (2015).
- K. Willquist, V. N. Nkemka, H. Svensson, S. Pawar, M. Ljunggren, H. Karlsson, M. Murto, C. Hulteberg, E. W. J. van Niel and G. Liden, Design of a novel biohythane process with high H_2 and CH_4 production rates, *Int. J. Hydrogen Energy*, **37**, 17749 (2012).
- S. Adhikari and S. Fernando, Hydrogen Membrane Separation Techniques, *Ind. Eng. Chem. Res.*, **45**, 875 (2006).
- R. Ge, X. Ren, F. Qu, D. Liu, M. Ma, S. Hao, G. Du, A. M. Asiri, L. Chen and X. Sun, Three-Dimensional Nickel-Borate Nanosheets Array for Efficient Oxygen Evolution at Near-Neutral pH, *Chem. - A Eur. J.*, **23**, 6959 (2017).
- X. Ren, R. Ge, Y. Zhang, D. Liu, D. Wu, X. Sun, B. Du and Q. Wei, Cobalt-borate nanowire array as a high-performance catalyst for oxygen evolution reaction in near-neutral media, *J. Mater. Chem. A*, **5**, 7291 (2017).
- N. W. Ockwig and T. M. Nenoff, Membranes for hydrogen separation, *Chem. Rev.*, **107**, 4078 (2007).
- K. Li, Ceramic Membranes for Separation and Reaction. John Wiley & Sons, Ltd, (2007).
- R. W. Baker, Gas Separation, in *Membrane Technology and Applications*, Third Edit., Chichester, UK: John Wiley & Sons, Ltd, (2012).
- H. Mirzaee and F. Mirzaee, Modeling and simulation gas separation by membrane of poly dimethyl siloxane, *J. King Saud Univ. - Eng. Sci.*, **24**, 35 (2012).
- B. Freeman and Y. Yampolskii, Eds., *Membrane Gas Separation*. John Wiley & Sons, Ltd, (2011).
- A. ten Bosch, A model for nanopore gas permeation, *Sep. Purif. Technol.*, **47**, 156 (2006).
- A. L. Mejdell, T. A. Peters, M. Stange, H. J. Venvik and R. Bredesen, Performance and application of thin Pd-alloy hydrogen separation membranes in different configurations, *J. Taiwan Inst. Chem. Eng.*, **40**, 253 (2009).
- M. E. E. Abashar, Ultra-clean hydrogen production by ammonia decomposition, *J. King Saud Univ. - Eng. Sci.*, (2016).
- H. W. Abu El Hawa, S. N. Paglieri, C. C. Morris, A. Harale and J. D. Way, Application of a Pd-Ru composite membrane to hydrogen production in a high temperature membrane reactor, *Sep. Purif. Technol.*, **147**, 388 (2015).
- F. Guazzone, J. Catalano, I. P. Mardilovich, J. Kniep, S. Pande, T. Wu, R. C. Lambrecht, S. Datta, N. K. Kazantzis and Y. H. Ma, Gas permeation field tests of composite Pd and Pd-Au membranes in actual coal derived syngas atmosphere, *Int. J. Hydrogen Energy*, **37**, 14557 (2012).
- O. Y. Abdelaziz, M. A. Gadalla and F. H. Ashour, Simulation of biomethanol production from green syngas through sustainable process design, in *Proceedings of the 4th International Conference on Simulation and Modeling Methodologies*,

- Technologies and Applications*, 677 (2014).
18. D. A. Ali, M. A. Gadalla, O. Y. Abdelaziz and F. H. Ashour, Modelling of coal-biomass blends gasification and power plant revamp alternatives in Egypt's natural gas sector, *Chem. Eng. Trans.*, **52**, 49 (2016).
 19. H. Lin, Z. He, Z. Sun, J. Vu, A. Ng, M. Mohammed, J. Kniep, T. C. Merkel, T. Wu and R. C. Lambrecht, CO₂-selective membranes for hydrogen production and CO₂ capture - Part I: Membrane development, *J. Memb. Sci.*, **457**, 149 (2014).
 20. H. Lin, Z. He, Z. Sun, J. Kniep, A. Ng, R. W. Baker and T. C. Merkel, CO₂-selective membranes for hydrogen production and CO₂ capture – Part II: Techno-economic analysis, *J. Memb. Sci.*, **493**, 794 (2015).
 21. M. M. Barreiro, M. Maroño and J. M. Sánchez, Hydrogen permeation through a Pd-based membrane and RWGS conversion in H₂/CO₂, H₂/N₂/CO₂ and H₂/H₂O/CO₂ mixtures, *Int. J. Hydrogen Energy*, **39**, 4710 (2014).
 22. H. Li, Z. Song, X. Zhang, Y. Huang, S. Li, Y. Mao, H. J. Ploehn, Y. Bao and M. Yu, Ultrathin, molecular-sieving graphene oxide membranes for selective hydrogen separation, *Science.*, **342**, no. 6154, 95 (2013).
 23. K. Briceño, A. Iulianelli, D. Montané, R. Garcia-Valls and A. Basile, Carbon molecular sieve membranes supported on non-modified ceramic tubes for hydrogen separation in membrane reactors,” *Int. J. Hydrogen Energy*, **37**, 13536 (2012).
 24. X. Ren, T. Zhang, D. Wu, T. Yan, X. Pang, B. Du, W. Lou and Q. Wei, Increased electrocatalyzed performance through high content potassium doped graphene matrix and aptamer tri infinite amplification labels strategy: Highly sensitive for matrix metalloproteinases-2 detection, *Biosens. Bioelectron.*, **94**, 694 (2017).
 25. H. Wang, Y. Zhang, Y. Wang, H. Ma, B. Du and Q. Wei, Facile synthesis of cuprous oxide nanowires decorated graphene oxide nanosheets nanocomposites and its application in label-free electrochemical immunosensor, *Biosens. Bioelectron.*, **87**, 745 (2017).
 26. D. Wu, Y. Liu, Y. Wang, L. Hu, H. Ma, G. Wang and Q. Wei, Label-free Electrochemiluminescent Immunosensor for Detection of Prostate Specific Antigen based on Aminated Graphene Quantum Dots and Carboxyl Graphene Quantum Dots, *Sci. Rep.*, **6**, no. 20511, (2016).
 27. X. Li, Y. Wang, L. Shi, H. Ma, Y. Zhang, B. Du, D. Wu and Q. Wei, A novel ECL biosensor for the detection of concanavalin A based on glucose functionalized NiCo₂S₄ nanoparticles-grown on carboxylic graphene as quenching probe, *Biosens. Bioelectron.*, **96**, 113 (2017).
 28. R. W. Baker, K. A. Lokhandwala, J. G. Wijmans and A. R. Da Costa, Nitrogen removal from natural gas using two types of membranes, U.S. Patent 6,630,011, (2003).
 29. A. A. Al-Rabiah, A. M. Ajbar, M. A. Soliman, F. A. Almalki and O. Y. Abdelaziz, Modeling of nitrogen separation from natural gas through nanoporous carbon membranes, *J. Nat. Gas Sci. Eng.*, **26**, 1278 (2015).
 30. Y. Jiang, Y. Wu, W. Wang, L. Li, Z. Zhou and Z. Zhang, Permeability and Selectivity of Sulfur Dioxide and Carbon Dioxide in Supported Ionic Liquid Membranes, *Chinese J. Chem. Eng.*, **17**, 594 (2009).
 31. Z. Wu, Z. Liu, W. Wang, Y. Fan and N. Xu, Diffusion of H₂, CO, N₂, O₂ and CH₄ Through Nanoporous Carbon Membranes, *Chinese J. Chem. Eng.*, **16**, 709 (2008).
 32. M. B. Rao and S. Sircar, Nanoporous carbon membranes for separation of gas mixtures by selective surface flow, *J. Memb. Sci.*, **85**, 253 (1993).
 33. M. B. Rao and S. Sircar, Nanoporous carbon membrane for gas separation, *Gas Sep. Purif.*, **7**, 279 (1993).
 34. A. M. Vieira-Linhares and N. A. Seaton, Non-equilibrium molecular dynamics simulation of gas separation in a microporous carbon membrane, *Chem. Eng. Sci.*, **58**, 4129 (2003).
 35. M. V. Sarfaraz, E. Ahmadpour, A. Salahi, F. Rekabdar and B. Mirza, Experimental investigation and modeling hybrid nano-porous membrane process for industrial oily wastewater treatment, *Chem. Eng. Res. Des.*, **90**, 1642 (2012).
 36. W. N. W. Salleh and A. F. Ismail, Carbon membranes for gas separation processes: Recent progress and future perspective, *J. Membr. Sci. Res.*, **1**, 2 (2015).
 37. M. B. Rao and S. Sircar, Performance and pore characterization of nanoporous carbon membranes for gas separation, *J. Memb. Sci.*, **110**, 109 (1996).
 38. Y. Shindo, T. Hakuta, H. Yoshitome and H. Inoue, Calculation Methods for Multicomponent Gas Separation by Permeation, *Sep. Sci. Technol.*, **20**, 445 (1985).
 39. M. A. Soliman, A spline collocation method for the solution of diffusion-convection problems with chemical reactions, *Chem. Eng. Sci.*, **47**, 4209 (1992).